A novel type of transient luminous event produced by terrestrial gamma-ray flashes

Wei Xu, Sébastien Celestin, Victor Pasko, Robert Marshall

AGU PUBLICATIONS

Geophysical Research Letters

RESEARCH LETTER
10.1002/2016GL072400

Key Points:
- Prediction of a novel type of transient luminous event produced by terrestrial gamma-ray flashes
- The predicted TLE is produced by TGF-induced electrons above cloud tops
- The spectroscopic, morphological, and temporal features of this luminous event are closely related with TGFs

Correspondence to:
W. Xu,
Wei-Xu@colorado.edu

Citation:
Xu, W., S. Celestin, V. P. Pasko, and R. A. Marshall (2017), A novel type of transient luminous event produced by terrestrial gamma-ray flashes, *Geophys. Res. Lett.*, *44*, 2571–2578, doi:10.1002/2016GL072400.

Received 19 DEC 2016
Accepted 14 FEB 2017
Accepted article online 15 FEB 2017
Published online 7 MAR 2017

A novel type of transient luminous event produced by terrestrial gamma-ray flashes

Wei Xu[1], Sebastien Celestin[2], Victor P. Pasko[3], and Robert A. Marshall[1]

[1]Department of Aerospace Engineering Sciences, University of Colorado Boulder, Boulder, Colorado, USA, [2]LPC2E, University of Orleans, CNRS, Orleans, France, [3]Communications and Space Sciences Laboratory, Department of Electrical Engineering, Pennsylvania State University, University Park, Pennsylvania, USA

Abstract Terrestrial Gamma-ray Flashes (TGFs), discovered in 1994 by the Compton Gamma-Ray Observatory, are high-energy photon bursts originating in the Earth's atmosphere in association with thunderstorms. In this paper, we demonstrate theoretically that, while TGFs pass through the atmosphere, the large quantities of energetic electrons knocked out by collisions between photons and air molecules generate excited species of neutral and ionized molecules, leading to a significant amount of optical emissions. These emissions represent a novel type of transient luminous events in the vicinity of the cloud tops. We show that this predicted phenomenon illuminates a region with a size notably larger than the TGF source and has detectable levels of brightness. Since the spectroscopic, morphological, and temporal features of this luminous event are closely related with TGFs, corresponding measurements would provide a novel perspective for investigation of TGFs, as well as lightning discharges that produce them.

1. Introduction

Thunderstorms occasionally behave as powerful particle accelerators and produce gamma-ray bursts with energies as high as a few tens of MeVs named terrestrial gamma-ray flashes (TGFs) [*Fishman et al.*, 1994]. This high-energy phenomenon has been extensively observed by low-orbit satellites: the Compton Gamma-Ray Observatory [*Fishman et al.*, 1994], the Reuven Ramaty High Energy Solar Spectroscopic Imager (RHESSI) [*Smith et al.*, 2005], the Fermi Gamma-Ray Space Telescope [*Briggs et al.*, 2010], and most recently by the Astrorivelatore Gamma a Immagini Leggero (AGILE) satellite [*Marisaldi et al.*, 2010]. Space-based measurements have revealed some temporal and spectral features of TGFs: they typically last from a fraction of to a few milliseconds, have a typical fluence slightly weaker than 1 photon/cm^2 when observed from a low-Earth orbit, and exhibit a hard energy spectrum extending up to a few tens of MeVs [e.g., *Smith et al.*, 2005; *Briggs et al.*, 2010; *Marisaldi et al.*, 2010]. In addition, detailed studies of TGF-associated lightning sferics have correlated this phenomenon with normal polarity intracloud lightning (+IC) that acts to transport negative charge upward within the cloud, specifically during the initial development stages [e.g., *Stanley et al.*, 2006; *Lu et al.*, 2010; *Shao et al.*, 2010]. It has also been proposed that the large number of runaway and secondary electrons involved in TGFs also radiate energetic radio signals [e.g., *Connaughton et al.*, 2013; *Dwyer and Cummer*, 2013], with amplitudes comparable with conventional lightning discharges. Moreover, through analyses of radio emissions, TGFs have been confirmed to be produced deep inside thunderstorms at an altitude of $\sim$12 km, with an intrinsic source brightness of $\sim 10^{18}$ runaway electrons [*Cummer et al.*, 2014].

The mechanism of relativistic runaway electron avalanche (RREA) [*Gurevich et al.*, 1992] has been found to reproduce the TGF cumulative energy spectrum observed by the RHESSI satellite [*Dwyer and Smith*, 2005]. Because the TGF fluence measured at satellite altitudes is too high to be explained solely by RREAs seeded from extensive air showers or natural background radiation, the positive feedback effects (X-rays and positrons) have been further suggested [*Dwyer*, 2008]. Modeling studies of relativistic feedback discharge (RFD) initiated by seed electrons from lightning leaders under thundercloud fields have shown that this mechanism can explain the observed properties of TGFs [*Dwyer*, 2012]. On the other hand, another mechanism on the basis of thermal runaway electrons produced by streamers during the negative corona flash of stepping lightning leaders has been proposed to be responsible for TGFs [*Moss et al.*, 2006; *Celestin and Pasko*, 2011]. Fluence and spectra of bremsstrahlung photons resulting from thermal runaway electrons after being accelerated by the electric field of the ascending negative leader in a high potential +IC lightning discharge agree with satellite measurements [e.g., *Xu et al.*, 2012; *Celestin et al.*, 2012, 2015].

Measurements of optical signals from TGF-associated IC flashes by the Lightning Imaging Sensor (LIS) have been reported [*Østgaard et al.*, 2013]. Although LIS cannot precisely determine the origin of these optical signals, motivated by these measurements, optical emissions originating from the impact excitation of air molecules by runaway electrons and their secondaries in TGFs have been theoretically quantified [*Dwyer et al.*, 2013; *Xu et al.*, 2015a]. While emitting intense bursts of gamma rays into space, the RFD has been suggested to produce weak but detectable, visible light intensities when compared with normal lightning [*Dwyer et al.*, 2013]. Moreover, it has been found that the TGF source of thermal runaway electrons accelerated at the tips of lightning leaders is accompanied with detectable levels of optical emissions [*Xu et al.*, 2015a]. Optical emissions reflect the intrinsic energetics and dynamics of electrons and can be used to investigate interaction of electron beams with neutral gas. *Lehtinen et al.* [2001] have proposed the measurements of fluorescence light in the geomagnetically conjugate ionosphere originating from energetic runaway electron beams (not necessarily associated with TGFs), after being produced by impulsive lightning discharges and propagating along the geomagnetic field lines, as means to explore electron properties. However, ground-based measurements of the optical signal in the conjugate hemisphere returned a null result [*Marshall et al.*, 2005]. Moreover, *Babich et al.* [2008] have calculated the air fluorescence energy based on the RREA mechanism for different source altitudes and found that TGFs are not necessarily correlated with blue jets or red sprites.

We show in this paper that the interaction of TGFs with the lower atmosphere would leave a detectable fluorescence trace in the vicinity of cloud tops. Before escaping the Earth's atmosphere, collisions of gamma rays with air molecules can give rise to large quantities of energetic electrons. A small portion of them, especially those produced at high altitudes ($\gtrsim$40 km), can be directly launched into the inner magnetosphere, becoming Terrestrial Electron Beams (TEBs) [*Dwyer et al.*, 2008]. The vast majority of the electrons produced by gamma-ray collisions at low altitude (<30 km) efficiently excite air molecules and generate a substantial number of excited neutral and ionized nitrogen molecules. Fluorescence photons are emitted with detectable levels in this case from very large ($\sim$10 km spatial extent) volumes of atmosphere via the radiative relaxation of these excited species. The fluorescence light, as well as accelerating runaway electrons and photon interactions with air molecules in TGFs, are schematically depicted in Figure 1a. In the following, we demonstrate that the large quantities of TGF-induced energetic electrons are sufficient to produce a distinctive novel type of transient luminous events (TLEs) [e.g., *Pasko*, 2010], regardless of the underlying TGF production mechanism.

2. Model Formulation

In this work, we mainly focus on optical emissions originating from the second positive band system of N_2 $\left(2PN_2, C^3\Pi_u \rightarrow B^3\Pi_g\right)$ and the first negative band system of N_2^+ $\left(1NN_2^+, B^2\Sigma_u^+ \rightarrow X^2\Sigma_g^+\right)$. N_2 $\left(C^3\Pi_u\right)$ and N_2^+ $\left(B^2\Sigma_u^+\right)$ are the upper excited states leading to $2PN_2$ and $1NN_2^+$ emissions, respectively. The upper excited states of $1PN_2$ emissions are heavily quenched at the production altitudes of TGFs [e.g., *Dwyer et al.*, 2013; *Xu et al.*, 2015a], and this band system is not considered. Optical emissions are quantified using a three-step procedure in the framework of Monte Carlo simulations. First, a Monte Carlo model is used to simulate photon transport during TGFs and the production of energetic electrons by gamma rays, including their production location and momentum. Second, we employ a Monte Carlo model for electrons to simulate their propagation in the atmosphere and the impact excitation of air molecules. Finally, the collisional quenching of excited species and the production of fluorescence photons are quantified using a model of optical emissions. Details about this suite of numerical models are discussed later in this paper.

The goal of the present study is to explore the properties of optical emissions produced by TGF-induced electrons independently of the exact source mechanism. For this goal, the TGF source is defined so that it provides quantitative results consistent with satellite measurements. Specifically, source photons have the characteristic energy distribution $f(\varepsilon)$ as would be produced by the bremsstrahlung radiation of RREAs: $f(\varepsilon) \propto \frac{\exp(-\varepsilon/\varepsilon_c)}{\varepsilon}$, where ε is the photon energy, ε_c is the high-energy cutoff of RREA energy distribution, and a typical value of 7 MeV is chosen for ε_c [e.g., *Dwyer and Smith*, 2005; *Carlson et al.*, 2007; *Dwyer et al.*, 2012]. As for the spatial distribution, it is assumed that these photons are uniformly distributed within a sphere with a characteristic radial dimension of 1 km [*Dwyer et al.*, 2012] at 12 km altitude [e.g., *Xu et al.*, 2012; *Cummer et al.*, 2014]. These photons are emitted upward using an isotropic beaming angle of 45° [e.g., *Dwyer and Smith*, 2005; *Carlson et al.*, 2007; *Xu et al.*, 2012].

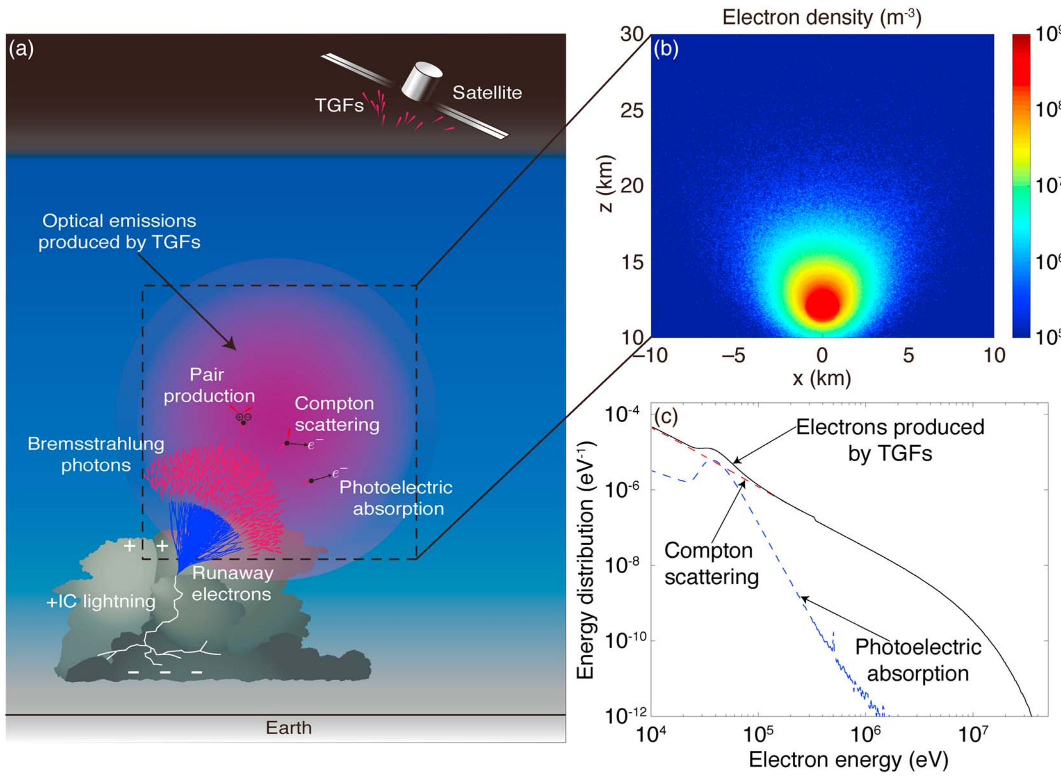

Figure 1. (a) Illustration of fluorescence light resulting from the radiative relaxation of excited species produced by the large fluxes of TGF-induced energetic electrons. (b) Cross-sectional view of the number density for electrons with energies above 10 keV knocked out during processes of photoelectric absorption and Compton scattering, while TGFs pass through the atmosphere. The results are obtained using a characteristic TGF source that provides quantitative results consistent with satellite measurements. (c) Energy distribution of electrons produced by TGFs in the altitude range between 10 and 30 km.

Recent radio measurements and modeling studies have revealed a deep (low altitude) source for TGFs [e.g., *Dwyer and Smith*, 2005; *Shao et al.*, 2010; *Lu et al.*, 2010; *Xu et al.*, 2012; *Cummer et al.*, 2014], and 10^{18} bremsstrahlung photons (with energy greater than 10 keV) are required in this case to agree with satellite measurements for a source altitude of 12 km [*Celestin et al.*, 2015]. This photon number is, therefore, adopted in the present work. Concerning the temporal distribution, we assume that the source of photons has a constant intensity with a duration of 200 μs [e.g., *Dwyer and Cummer*, 2013; *Fishman et al.*, 2011; *Gjesteland et al.*, 2010]. As estimated from Fermi measurements of TGF pulses, the durations of the TGF sources can range from ~50 μs to ~0.5 ms [*Fishman et al.*, 2011]. With the dead time effects taken into account, analyses of Burst and Transient Source Experiment measurements have indicated a typical duration of 250 μs for TGF production [*Gjesteland et al.*, 2010]. Variation in the duration and fluence of the TGF source would lead to a proportional change in the production rate of bremsstrahlung photons and modeling results on the luminosities of optical emissions. It is important to note that analysis of Fermi measurements have suggested that the intrinsic duration of TGFs could be much shorter than previously observed [*Briggs et al.*, 2013; *Fitzpatrick et al.*, 2014]. With reduced dead time effects, AGILE measurements have also revealed TGF events briefer than 100 μs [*Marisaldi et al.*, 2015]. Therefore, it is likely that the true duration of TGF source could be notably shorter than 200 μs. In that case, the brightness of TGF-induced luminous event would become proportionally higher than that found in the present work (Figure 2).

We simulate photon transport in the Earth's atmosphere, along with the production of energetic electrons via collisions of gamma rays with air molecules, using a Monte Carlo model. Based on previously published modeling studies [*Østgaard et al.*, 2008], this model takes into account three types of photon collisions that are dominant in the energy range between 10 keV and 100 MeV: photoelectric absorption, Compton scattering, and electron-positron pair production. The bremsstrahlung radiation of energetic electrons produced by TGFs is not considered. It has been validated by calculating the energy spectra as would be measured by satellites

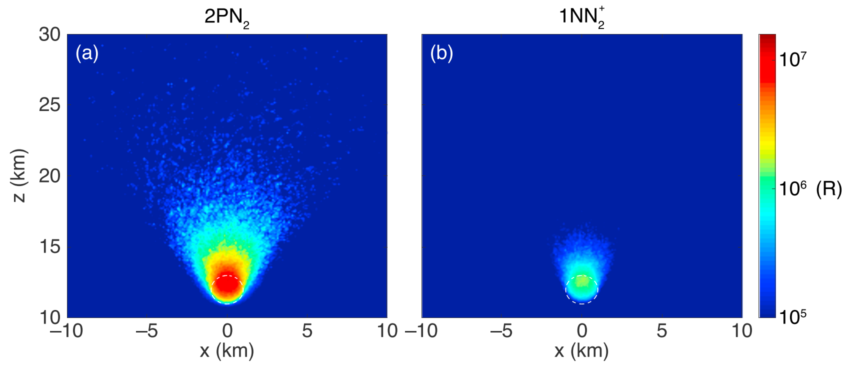

Figure 2. Optical emissions of (a) $2PN_2$ and (b) $1NN_2^+$ produced by the fluxes of TGF-induced electrons via impact excitations of air molecules. The dashed lines represent the spherical spatial distribution assumed for source photons in TGFs. The results are calculated using a convolution technique and a characteristic TGF source, with a duration of 200 μs and 10^{18} photons with energy greater than 10 keV.

in the theory of TGF production by RREAs. Modeling results show excellent agreement with previously published data [*Xu et al.*, 2012]. Concerning the production of electrons, the electron binding energy is neglected in the process of photoelectric absorption and the outgoing photoelectron is assumed to have the same energy as the incident photon. The photoelectron momentum is determined using the relativistic form of the analytical angular differential cross section for photoelectric absorption processes [*Davisson and Evans*, 1952]. As for the Compton scattering, the energy and momentum of the electron knocked out are obtained using the conservation of momentum and energy.

We use another Monte Carlo model to simulate the propagation of electrons and their collisions with air molecules (80% N_2 and 20% O_2). This model is three-dimensional (3-D) in both velocity and configuration space. It is capable of simulating electrons under an electromagnetic field for energies between sub-eV and GeV [*Celestin and Pasko*, 2011]. This model has been validated through various comparisons with results calculated using other numerical models for both low [*Hagelaar and Pitchford*, 2005] and high [*Dwyer et al.*, 2012] energy range [*Xu et al.*, 2015a]. The initial location and momenta of electrons knocked out during collisions of gamma rays with air molecules are taken directly from Monte Carlo simulation of photon transport. The production of these electrons occurs far away from the TGF source (see Figure 1b), and we neglect, in this study, the electric field giving rise to the acceleration of runaway electrons producing the TGF itself. Indeed, in the present work, we focus on the fluorescence emission produced above cloud tops. Taking into account the electric field would only enhance the fluorescence emissions produced by accelerating TGF-induced electrons in the source, i.e., within the cloud. The geomagnetic field is assumed to be uniform and horizontal with a magnitude of 50 μT. The lower energy limit of the simulated electrons is set to be 10 eV in order to ensure accurate modeling of the production of upper excited states of $2PN_2$ and $1NN_2^+$. As a result, this model can fully simulate the dynamics of both high- and low-energy electrons, and the production of fluorescence photons from $2PN_2$ and $1NN_2^+$. Cross sections used for modeling the excitation of $N_2(C^3\Pi_u)$ are taken from the BOLSIG+ database [*Hagelaar and Pitchford*, 2005]. As for the production of $N_2^+\left(B^2\Sigma_u^+\right)$, we use the relativistic binary-encounter-Bethe model [e.g., *Kim et al.*, 2000; *Celestin and Pasko*, 2010], which provides an orbital description of the cross section for ionizing $\left(2\sigma_u\right)$ electrons of nitrogen molecules [e.g., *Van Zyl and Pendleton*, 1995].

At the typical altitudes of TGF source, $N_2\left(C^3\Pi_u\right)$ and $N_2^+\left(B^2\Sigma_u^+\right)$ are produced through direct impact excitations and are mostly depopulated by collisions of excited species with neutral air molecules. For the sake of exploring morphological features, we discretize the region where energetic electrons are produced using a Cartesian grid of 201×201×201 grid cells, spanning 20 km in *x* and *y* directions, and an altitude range between 10 km and 30 km. For each numerical cell, the production of upper excited states of $2PN_2$ and $1NN_2^+$, including the time and location of production, is directly determined by Monte Carlo simulations. The deexcitation of excited species is simulated using another optical emission model. In particular, $N_2\left(C^3\Pi_u\right)$ is considered to be quenched by collisions with N_2 molecules, with a rate coefficient of 10^{-11} cm^3/s, and O_2 molecules, with a rate coefficient of 3×10^{-10} cm^3/s [*Xu et al.*, 2015a]. $N_2^+\left(B^2\Sigma_u^+\right)$ can be deactivated by collisions with N_2 and O_2 molecules, with rate coefficients of 4.53×10^{-10} cm^3/s and 7.36×10^{-10} cm^3/s [*Kuo et al.*, 2005; *Xu et al.*, 2015a], respectively. The effects of radiative transfer between the observer and the source of emission are not considered in this study. We emphasize that results of fluorescence efficiency calculated using this optical emission model are in good agreement with laboratory experiments [*Xu et al.*, 2015a].

The lifetimes of upper excited states $\left(N_2\left(C^3\Pi_u\right)\text{ and }N_2^+\left(B^2\Sigma_u^+\right)\right)$ responsible for optical emissions from $2PN_2$ and $1NN_2^+$ depend on processes of collisional quenching. At TGF source altitudes, these lifetimes are on the order of nanoseconds, while TGFs have a duration on the order of hundred microseconds. As a consequence, a steady state of optical emissions would be established by the continuous excitation of air molecules, and in the present work, optical emissions are quantified using a convolution technique [e.g., *Xu et al.*, 2015b]. Rather than directly modeling the continuous production of bremsstrahlung photons, we assume that these photons are produced simultaneously at $t=0$ in the atmosphere. The time-resolved fluorescence beam and the impulse response of the system are further calculated. The steady state of optical emissions is finally derived by performing a time convolution of this impulse response with the continuous source using the production rate (assumed constant for 200 μs in this work) of bremsstrahlung photons.

3. Results

Figure 1b shows numerical modeling results of the density of electrons knocked out during processes of photoelectric absorption and Compton scattering, as TGFs traverse the atmosphere. TGF-induced electrons are mostly distributed in the altitude range below 20 km, roughly within a sphere with a radial dimension of ~4 km. Moreover, a characteristic photon in a TGF, before being absorbed or before escaping the atmosphere, is capable of generating on average approximately 4.4 electrons with energies above 10 keV. The maximum electron density found in our simulation is $\sim 4.8\times10^8$ m^{-3}. It is interesting to note that the density of electrons arising from TGFs, although less energetic and distributed over a larger volume, is comparable to that of runaway electrons producing TGFs. Indeed, a typical density of runaway electrons in TGFs would be $\sim 2.4\times10^8$ m^{-3}, if one considers that a total of 10^{18} runaway electrons [e.g., *Cummer et al.*, 2014; *Dwyer et al.*, 2012] are uniformly distributed within a sphere with a radius of 1 km [*Dwyer et al.*, 2012]. Note that electrons resulting from electron-positron pair production are not taken into account in the present work because the average number of electron-positron pairs produced per gamma ray is ~0.017. Modeling of electron-positron pair production is simplified by assuming that the positron annihilates locally and two photons with energy of 511 keV are produced. The pair-produced electron is not considered. We note that this assumption could underestimate the total energy deposition into the atmosphere, as well as the total fluorescence energy, by not more than 16%, as estimated from preliminary simulations.

Figure 1c shows the averaged energy distribution in the range above 10 keV for those electrons produced by TGFs at altitudes between 10 and 30 km. The integration of this distribution (solid line) over electron energy is equal to one. In order to emphasize the difference in electron energetics, we have presented separately the energy distributions for photoelectric absorption and Compton scattering as dashed lines. The integration of each partial distribution over electron energy is the fraction of electrons knocked out during a given process with respect to the total number of electrons produced. The average energy of these TGF-induced electrons is ~187 keV. Using a total number of 4.4×10^{18}, the energy deposited by this ensemble of electrons into the atmosphere is found to be ~0.13 MJ, accounting for ~82% of the total energy of the TGF source photons.

Figures 2a and 2b show, respectively, estimated optical emissions from $2PN_2$ and $1NN_2^+$ produced by the fluxes of TGF-induced electrons via impact excitations of air molecules. The dashed circles represent the spherical spatial distribution assumed for the TGF source. We note that modeling results of optical emissions, especially the intensity, depend on the choice of production rate for bremsstrahlung photons, specifically on the brightness and duration of TGF source. Present results are obtained by considering that total 10^{18} photons [*Celestin et al.*, 2015] are produced by a source with a constant intensity of 5×10^{21} photons/s remaining active for 200 μs [*Dwyer and Cummer*, 2013; *Fishman et al.*, 2011; *Gjesteland et al.*, 2010]. As shown in Figure 2, the maximum intensities of $2PN_2$ and $1NN_2^+$ are 11.2 MR and 1.6 MR, respectively. For the sake of estimating the brightness in the visible wavelength range (390–700 nm), we have used the aurora spectra to approximate the spectral distribution of fluorescence photons [*Dwyer et al.*, 2013] and the intensities are found to be ~1.2 MR and ~1.5 MR for $2PN_2$ and $1NN_2^+$, respectively. The intensity ratio of $2PN_2$ to $1NN_2^+$ in the visible wavelength range is ~0.8. Moreover, the fluorescence beam exhibits a fan-shaped structure with a diameter of ~6 km, which resembles the beaming geometry assumed for the TGF source. This beam appears to be notably larger than the TGF source, and the brightest spot is not exactly collocated with the center of TGF source. Note that the effect of the Earth's magnetic field on the shape of this fluorescence beam is insignificant because, for typical TGF-induced electrons, collisions with air molecules play a dominant role in the electron motion at this altitude.

4. Discussion

It is important to emphasize that the luminosity accompanying runaway electrons in TGF sources [*Dwyer et al.*, 2013; *Xu et al.*, 2015a], as well as that from the ascending intracloud lightning leader, is obscured by the thundercloud. However, the luminous event reported herein extends outside the thundercloud, thereby facilitating the observation by ground-based instruments. Depending on the latitude, thundercloud tops are approximately in the range ∼12–15 km. One clearly sees from Figure 2 that the intensity of optical emissions at an altitude of 17 km, i.e., 5 km away from the TGF source and above the cloud tops, is on the order of a fraction of MR. Concerning the color of this luminous event, it is mainly blue, primarily covering wavelengths from 300 to 430 nm of $2PN_2$ and $1NN_2^+$ band systems. Thus, it is spectrally distinguishable from the scattered light from lightning discharges. Note that *Stolzenburg et al.* [2016] have identified luminosity increases that might be associated with TGFs during the initial breakdown stages of lightning flashes that emitted radio signals similar to those producing TGFs. Moreover, since the production of electrons and excitation of air molecules are directly controlled by bremsstrahlung photons, the time dynamics of this event closely follows that of the TGF source.

The intensity of this luminous event is on the order of MR at the altitude of TGFs. This luminosity is close to the brightness of blue starters in the same altitude range [*Wescott et al.*, 2001] but an order of magnitude weaker than sprite streamer heads in the *D* region of ionosphere [*Qin et al.*, 2013]. Given the above mentioned location, size, and intensity, this luminous event is likely detectable. Furthermore, the morphological and spectroscopic features of this predicted type of TLEs are closely associated with the source properties of TGFs. First, the size and intensity of this fluorescence event are determined by the brightness and beaming of the TGF source. Second, this optical output reflects the intrinsic energy distribution of TGF-induced electrons, which is controlled by the energetics of TGF source. Hence, corresponding measurements would provide a novel perspective to investigate TGFs, as well as the initial breakdown stages of IC flashes.

To confirm the predicted brightness of the new luminous event (Figure 2), we can also quantify the intensity of these optical emissions using fluorescence efficiencies, similar to calculation of optical emissions from extensive air showers produced by ultrahigh-energy cosmic rays [*Nagano et al.*, 2004; *Xu et al.*, 2015a]. We note that this method has been applied to estimate optical emissions directly produced by theoretical relativistic feedback discharges [*Dwyer et al.*, 2013]. Fluorescence efficiency is an experimentally identified quantity that describes the fraction of the total energy deposition by electrons that is transferred into fluorescence emissions. Its value for $2PN_2$ and $1NN_2^+$ in the visible wavelength range without considering collisional quenching is approximately 0.0312% and 0.46% [*Dwyer et al.*, 2013], respectively. Knowing the total energy deposition and the effects of collisional deexcitation at the altitude of 12 km, the fluorescence energy is found to be ∼1.8 J and ∼2.6 J for $2PN_2$ and $1NN_2^+$, respectively. The average energy of fluorescence photons with visible wavelengths from $2PN_2$ and $1NN_2^+$ estimated using measurements of aurora spectra [*Dwyer et al.*, 2013] is 3 eV and 3.1 eV, respectively. This fluorescence energy corresponds to a production of 3.75×10^{18} and 5.24×10^{18} photons from $2PN_2$ and $1NN_2^+$. If we consider that these fluorescence photons have the same duration as the causative TGF (200 μs) and a uniform spherical and isotropic distribution with a radius of ∼3 km (see Figure 2), the intensities would be 2.1×10^5 R and 2.9×10^5 R, respectively, for $2PN_2$ and $1NN_2^+$ in the visible wavelength range. These luminosities agree well with the average luminosity of present modeling results (see Figure 2).

Unlike previously reported optical emissions associated with runaway electrons [*Dwyer et al.*, 2013; *Xu et al.*, 2015a], the luminous event modeled in this paper is spatially separated from the TGF-producing lightning discharge. This is because the attenuation length of relativistic electrons is much shorter than gamma rays [*Suszcynsky et al.*, 1996]. For example, a typical value for the attenuation length of 1 MeV electrons in the ambient air density at 12 km is ∼16 m [*Suszcynsky et al.*, 1996], while it is ∼511 m for 1 MeV photons [*Suszcynsky et al.*, 1996]. In the theory of TGF production by stepping lightning leaders, thermal runaway electrons are accelerated in a compact region (∼500 m at 12 km [*Celestin et al.*, 2015]) around a lightning leader tip. As a result of the longer attenuation length of gamma rays, secondary electrons produced during the transport of gamma rays are dissipated over a region up to a few kilometers away from the TGF source. This region, later illuminated by TGF-produced fluorescence light, is significantly larger than the avalanche region of runaway electrons. Additionally, optical emissions produced by TGFs are much weaker in terms of brightness and temporally successive to those arising from runaway electrons. The intensity ratio of $2PN_2$ to $1NN_2^+$ in the visible wavelength range is found to be ~0.8 for the luminous event produced by TGFs. We note that this value is close to TGF production by stepping lightning leaders, as well as RREAs developed in a large-scale homogeneous electric field with a magnitude of 4.3 kV/cm [*Xu et al.*, 2015a].

X-ray bursts from natural cloud-to-ground lightning and TGFs have been explained on the basis of production of thermal runaway electrons during the negative corona flash stage of stepping lightning leaders [*Celestin et al.*, 2015]. It has also been pointed out that TGFs represent a small fraction of lightning-leader-produced gamma-ray radiation [e.g., *Celestin et al.*, 2015; *Østgaard et al.*, 2012]. The mechanism of fluorescence production described in the present work naturally occurs in the atmosphere with the presence of large quantities of energetic X-rays and gamma rays. It is thus conceivable that this mechanism is also applicable to lightning leaders that would not be capable of producing gamma rays detectable from space. As long as these lightning-leader-produced gamma rays are sufficiently energetic and dense, considerable amounts of fluorescence light would be produced in the vicinity of cloud tops. We expect that the observation of the predicted TLEs would lead to significant improvement of the understanding of TGFs, particularly concerning their occurrence frequencies, time dynamics, source geometry, energetics, their relation with lightning discharges, and more generally of their role in the atmosphere-ionosphere-magnetosphere system.

Acknowledgments
This research was supported by the NSF grants AGS-1106779 and AGS-1243176. Sebastien Celestin's research is supported by the French Space Agency (CNES) in the framework of the space mission TARANIS. All data used in this paper are directly available after a request is made to authors W.X. (Wei-Xu@colorado.edu), S.C. (sebastien.celestin@cnrs-orleans.fr), V.P.P. (vpasko@psu.edu), or R.A.M. (Robert.Marshall@colorado.edu).

References

Babich, L. P., E. N. Donskoy, and I. M. Kutsyk (2008), Analysis of atmospheric gamma-ray flashes detected in near space with allowance for the transport of photons in the atmosphere, *J. Exp. Theor. Phys.*, *107*, 49–60.
Briggs, M. S., et al. (2010), First results on terrestrial gamma ray flashes from the Fermi Gamma-ray Burst Monitor, *J. Geophys. Res.*, *115*, A07323, doi:10.1029/2009JA015242.
Briggs, M. S., et al. (2013), Terrestrial gamma-ray flashes in the Fermi era: Improved observations and analysis methods, *J. Geophys. Res. Space Physics*, *118*, 3805–3830, doi:10.1002/jgra.50205.
Carlson, B. E., N. G. Lehtinen, and U. S. Inan (2007), Constraints on terrestrial gamma ray flash production from satellite observation, *Geophys. Res. Lett.*, *34*, L08809, doi:10.1029/2006GL029229.
Celestin, S., and V. P. Pasko (2010), Soft collisions in relativistic runaway electron avalanches, *J. Phys. D: Appl. Phys.*, *43*, 315206, doi:10.1088/0022-3727/43/31/315206.
Celestin, S., and V. P. Pasko (2011), Energy and fluxes of thermal runaway electrons produced by exponential growth of streamers during the stepping of lightning leaders and in transient luminous events, *J. Geophys. Res.*, *116*, A03315, doi:10.1029/2010JA016260.
Celestin, S., W. Xu, and V. P. Pasko (2012), Terrestrial gamma ray flashes with energies up to 100 MeV produced by nonequilibrium acceleration of electrons in lightning, *J. Geophys. Res.*, *117*, A05315, doi:10.1029/2012JA017535.
Celestin, S., W. Xu, and V. P. Pasko (2015), Variability in fluence and spectrum of high-energy photon bursts produced by lightning leaders, *J. Geophys. Res. Space Physics*, *120*, 10,712–10,723, doi:10.1002/2015JA021410.
Connaughton, V., et al. (2013), Radio signals from electron beams in terrestrial gamma ray flashes, *J. Geophys. Res. Space Physics*, *118*, 2313–2320, doi:10.1029/2012JA018288.
Cummer, S. A., M. S. Briggs, J. R. Dwyer, S. Xiong, V. Connaughton, G. J. Fishman, G. Lu, F. Lyu, and R. Solanki (2014), The source altitude, electric current, and intrinsic brightness of terrestrial gamma ray flashes, *Geophys. Res. Lett.*, *41*, 8586–8593, doi:10.1002/2014GL062196.
Davisson, C. M., and R. D. Evans (1952), Gamma-ray absorption coefficients, *Rev. Mod. Phys.*, *24*, 79–107.
Dwyer, J. R. (2008), Source mechanisms of terrestrial gamma-ray flashes, *J. Geophys. Res.*, *113*, D10103, doi:10.1029/2007JD009248.
Dwyer, J. R. (2012), The relativistic feedback discharge model of terrestrial gamma ray flashes, *J. Geophys. Res.*, *117*, A02308, doi:10.1029/2011JA017160.
Dwyer, J. R., and S. A. Cummer (2013), Radio emissions from terrestrial gamma-ray flashes, *J. Geophys. Res. Space Physics*, *118*, 3769–3790, doi:10.1002/jgra.50188.
Dwyer, J. R., and D. M. Smith (2005), A comparison between Monte Carlo simulations of runaway breakdown and terrestrial gamma-ray flash observations, *Geophys. Res. Lett.*, *32*, L22804, doi:10.1029/2005GL023848.
Dwyer, J. R., B. W. Grefenstette, and D. M. Smith (2008), High-energy electron beams launched into space by thunderstorms, *Geophys. Res. Lett.*, *35*, L02815, doi:10.1029/2007GL032430.
Dwyer, J. R., D. M. Smith, and S. A. Cummer (2012), High-energy atmospheric physics: Terrestrial gamma-ray flashes and related phenomena, *Space Sci. Rev.*, *173*, 133–196, doi:10.1007/s11214-012-9894-0.
Dwyer, J. R., N. Y. Liu, and H. K. Rassoul (2013), Properties of the thundercloud discharges responsible for terrestrial gamma-ray flashes, *Geophys. Res. Lett.*, *40*, 4067–4073, doi:10.1002/grl.50742.
Fishman, G. J., et al. (1994), Discovery of intense gamma-ray flashes of atmospheric origin, *Science*, *264*(5163), 1313–1316.
Fishman, G. J., et al. (2011), Temporal properties of the terrestrial gamma-ray flashes from the Gamma-Ray Burst Monitor on the Fermi Observatory, *J. Geophys. Res.*, *116*, A07304, doi:10.1029/2010JA016084.
Fitzpatrick, G., et al. (2014), Compton scattering in terrestrial gamma-ray flashes detected with the Fermi gamma-ray burst monitor, *Phys. Rev. D*, *90*, 043008, doi:10.1103/PhysRevD.90.043008.
Gjesteland, T., N. Østgaard, P. H. Connell, J. Stadsnes, and G. J. Fishman (2010), Effects of dead time losses on terrestrial gamma ray flash measurements with the Burst and Transient Source Experiment, *J. Geophys. Res.*, *115*, A00E21, doi:10.1029/2009JA014578.
Gurevich, A. V., G. M. Milikh, and R. A. Roussel-Dupré (1992), Runaway electron mechanism of air breakdown and preconditioning during a thunderstorm, *Phys. Lett. A*, *165*(5–6), 463–468, doi:10.1016/0375-9601(92)90348-P.
Hagelaar, G. J. M., and L. C. Pitchford (2005), Solving the Boltzmann equation to obtain electron transport coefficients and rate coefficients for fluid models, *Plasma Sources Sci. Technol.*, *14*, 722–733, doi:10.1088/0963-0252/14/4/011.

Kim, Y.-K., J. P. Santos, and F. Parente (2000), Extension of the binary-encounter-dipole model to relativistic incident electrons, *Phys. Rev. A*, *62*(052710), doi:10.1103/PhysRevA.62.052710.

Kuo, C.-L., R. R. Hsu, A. B. Chen, H. T. Su, L. C. Lee, S. B. Mende, H. U. Frey, H. Fukunishi, and Y. Takahashi (2005), Electric fields and electron energies inferred from the ISUAL recorded sprites, *Geophys. Res. Lett.*, *32*, L19103, doi:10.1029/2005GL023389.

Lehtinen, N. G., U. S. Inan, and T. F. Bell (2001), Effects of thunderstorm-driven runaway electrons in the conjugate hemisphere: Purple sprites, ionization enhancements, and gamma rays, *J. Geophys. Res.*, *106*(A12), 28,841–28,856, doi:10.1029/2000JA000160.

Lu, G., R. J. Blakeslee, J. Li, D. M. Smith, X.-M. Shao, E. W. McCaul, D. E. Buechler, H. J. Christian, J. M. Hall, and S. A. Cummer (2010), Lightning mapping observation of a terrestrial gamma-ray flash, *Geophys. Res. Lett.*, *37*, L11806, doi:10.1029/2010GL043494.

Marisaldi, M., et al. (2010), Detection of terrestrial gamma ray flashes up to 40 MeV by the AGILE satellite, *J. Geophys. Res.*, *115*, A00E13, doi:10.1029/2009JA014502.

Marisaldi, M., et al. (2015), Enhanced detection of terrestrial gamma-ray flashes by AGILE, *Geophys. Res. Lett.*, *42*, 9481–9487, doi:10.1002/2015GL066100.

Marshall, R. A., et al. (2005), Optical observations geomagnetically conjugate to sprite-producing lightning discharges, *Ann. Geophys.*, *23*, 2231–2237.

Moss, G. D., V. P. Pasko, N. Liu, and G. Veronis (2006), Monte Carlo model for analysis of thermal runaway electrons in streamer tips in transient luminous events and streamer zones of lightning leaders, *J. Geophys. Res.*, *111*, A02307, doi:10.1029/2005JA011350.

Nagano, M., K. Kobayakawa, N. Sakaki, and K. Ando (2004), New measurement on photon yields from air and the application to the energy estimation of primary cosmic rays, *Astropart. Phys.*, *22*, 235–248, doi:10.1016/j.astropartphys.2004.08.002.

Østgaard, N., T. Gjesteland, J. Stadsnes, P. H. Connell, and B. Carlson (2008), Production altitude and time delays of the terrestrial gamma flashes: Revisiting the Burst and Transient Source Experiment spectra, *J. Geophys. Res.*, *113*, A02307, doi:10.1029/2007JA012618.

Østgaard, N., T. Gjesteland, R. S. Hansen, A. B. Collier, and B. Carlson (2012), The true fluence distribution of terrestrial gamma flashes at satellite altitude, *J. Geophys. Res.*, *117*, A03327, doi:10.1029/2011JA017365.

Østgaard, N., T. Gjesteland, B. E. Carlson, A. B. Collier, S. A. Cummer, G. Lu, and H. J. Christian (2013), Simultaneous observations of optical lightning and terrestrial gamma ray flash from space, *Geophys. Res. Lett.*, *40*, 2423–2426, doi:10.1002/grl.50466.

Pasko, V. P. (2010), Recent advances in theory of transient luminous events, *J. Geophys. Res.*, *115*, A00E35, doi:10.1029/2009JA014860.

Qin, J., S. Celestin, V. P. Pasko, S. A. Cummer, M. G. McHarg, and H. C. Stenbaek-Nielsen (2013), Mechanism of column and carrot sprites derived from optical and radio observations, *Geophys. Res. Lett.*, *40*, 4777–4782, doi:10.1002/grl.50910.

Shao, X.-M., T. Hamlin, and D. M. Smith (2010), A closer examination of terrestrial gamma-ray flash-related lightning processes, *J. Geophys. Res.*, *115*, A00E30, doi:10.1029/2009JA014835.

Smith, D. M., L. I. Lopez, R. P. Lin, and C. P. Barrington-Leigh (2005), Terrestrial gamma-ray flashes observed up to 20 MeV, *Science*, *307*(5712), 1085–1088.

Stanley, M. A., X.-M. Shao, D. M. Smith, L. I. Lopez, M. B. Pongratz, J. D. Harlin, M. Stock, and A. Regan (2006), A link between terrestrial gamma-ray flashes and intracloud lightning discharges, *Geophys. Res. Lett.*, *33*, L06803, doi:10.1029/2005GL025537.

Stolzenburg, M., T. C. Marshall, S. Karunarathne, and R. E. Orville (2016), Luminosity with intracloud-type lightning initial breakdown pulses and terrestrial gamma-ray flash candidates, *J. Geophys. Res. Atmos.*, *121*, 10,919–10,936, doi:10.1002/2016JD025202.

Suszcynsky, D. M., R. Roussel-Dupre, and G. Shaw (1996), Ground-based search for X rays generated by thunderstorms and lightning, *J. Geophys. Res.*, *101*(D18), 23,505–23,516, doi:10.1029/96JD02134.

Van Zyl, B., and W. Pendleton Jr. (1995), $N_2^+(X)$, $N_2^+(A)$, and $N_2^+(B)$ production in $e^- + N_2$ collisions, *J. Geophys. Res.*, *100*(A12), 23,755–23,762, doi:10.1029/95JA02699.

Wescott, E. M., D. D. Sentman, H. C. Stenbaek-Nielsen, P. Huet, M. J. Heavner, and D. R. Moudry (2001), New evidence for the brightness and ionization of blue starters and blue jets, *J. Geophys. Res.*, *106*(A10), 21,549–21,554, doi:10.1029/2000JA000429.

Xu, W., S. Celestin, and V. P. Pasko (2012), Source altitudes of terrestrial gamma-ray flashes produced by lightning leaders, *Geophys. Res. Lett.*, *39*, L08801, doi:10.1029/2012GL051351.

Xu, W., S. Celestin, and V. P. Pasko (2015a), Optical emissions associated with terrestrial gamma ray flashes, *J. Geophys. Res. Space Physics*, *120*, 1355–1370, doi:10.1002/2014JA020425.

Xu, W., S. Celestin, and V. P. Pasko (2015b), Optical emissions associated with energetic electrons produced by stepping leaders in cloud-to-ground lightning discharges, *Geophys. Res. Lett.*, *42*, 5610–5616, doi:10.1002/2015GL064419.